



Dedicated to Dr. Maria Zaharescu
on the occasion of her 80th anniversary

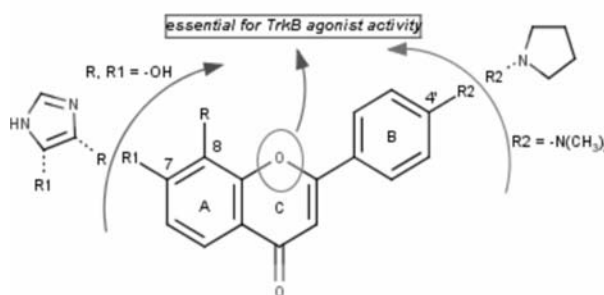
THEORETICAL STUDY OF SOME 7,8-DYHYDROXYFLAVONE ANALOGUES AS TROPOMYOSIN-RELATED KINASE B AGONISTS**

Alina BORA, Sorin AVRAM, Ana BOROTA, Ramona CURPAN and Liliana HALIP*

Institute of Chemistry Timișoara of Roumanian Academy, Computational Chemistry Department, 24 Mihai Viteazul, 300223 Timișoara, Roumania

Received July 31, 2017

7,8-Dihydroxyflavone, a small molecular tropomyosin-related kinase B (TrkB) receptor agonist belongs to the family of flavonoids and shares many of their properties. In the present study, Density Functional Theory based global reactivity descriptors are used to understand the relationship between structure, stability, global chemical reactivity and their responsibility for agonistic activity of the 7,8-dihydroxyflavone and its analogs. In this light, the heat of formation, Fukui indices, HOMO-LUMO gap, hardness, softness, electronegativity, and electrophilicity index have been computed. Our results showed that 7,8-dihydroxy groups (on the A ring) and the oxygen atom (in the middle of C ring) are essential for the agonistic effect. Additionally, to the electronic molecular properties, we discuss the pharmacokinetic profile of these derivatives. Hence, the theoretical results support the available experimental information regarding the key roles of catechol group for the flavonoids agonistic activity.



INTRODUCTION

Flavonoids are a group of over 9000 naturally bioactive polyphenolic compounds widely distributed in fruits and vegetables, fulfilling many biological properties including antioxidant, anti-inflammatory, and anti-carcinogenic effects. Their natural origin, high efficiency, low toxicity and important effects on cancer chemoprevention and chemotherapy indicate flavonoids as of great practical and theoretical importance.¹⁻⁴

Various investigation of flavonoids at the theoretical and experimental level suggested that small chemical modifications on the flavonoid core can have significant effects on their biological activity, metabolism, and bioavailability. These

chemical modifications could be related to the total number of hydroxyl groups, the configuration, the substitution and/or the arrangement of functional groups.^{1,5,6} These remarks increased interest to evaluate the key functional groups of the flavonoid structure which influence the activity and the pharmacokinetic profile. The general structure of flavonoids consists of two or more aromatics rings (the A and B rings) connected by a third pyranic ring (the C ring), (Fig. 1). Based on the variation in the heterocyclic C-ring, flavonoids are divided into seven major subgroups including flavones, flavonols, flavanones, flavanonols, flavanols or catechins, anthocyanins, and chalcones.^{7,8} 7,8-Dihydroxyflavone (7,8-DHF), a small molecular tropomyosin-related kinase B receptor (TrkB) agonist belongs to

* Corresponding author: lili.ostopovici@gmail.com

** Supplementary Information on <http://web.icf.ro/rrech/> or <http://revroum.lew.ro/>

the family of flavonoids and shares many of their properties. 7,8-DHF was found to be a potent mimic of brain-derived neurotrophic factor (BDNF) which acts on TrkB in a similar manner. This is associated with the possibility of 7,8-DHF to cause similar effects as BDNF in the brain.⁹ Theoretically, 7,8-DHF could be more therapeutically useful due to its better absorption and capacity to cross the blood-brain barrier (BBB).^{9,10} There are few experimental studies which confirm the importance of 7,8-dihydroxy groups attached to the catechol skeleton for the TrkB agonistic effect. Due to the relatively poor pharmacokinetic profile of the catechol-containing molecules and for increasing the TrkB agonistic activity, researcher synthesized and experimentally tested various 7,8-DHF derivatives.^{11,12} To the best of our knowledge, most of the theoretical studies are reported only for single 7,8-DHF compound without relating them to the whole 7,8-DHF analogs which displayed TrkB agonistic effect.¹³ Owing to flavonoids importance in human health, the detailed knowledge of their molecular structures, both from energetic and geometric viewpoints, appears to be essential for the development of novel chemotherapeutic agents with the improved physicochemical profile. In this regard, computational chemistry in conjunction with experimental results is one of the most powerful tools which provides valuable information at reduced time-consuming and economic costs and increases the drug discovery process.

The present research investigates, at theoretically level, the structural and electronic properties of 7,8-DHF and five analogues by performing semiempirical molecular orbital theory at the level AM1 and density functional theory quantum chemical (DFT) calculations. Additionally, to the electronic molecular properties (heat of formation, Fukui indices, HOMO-LUMO gap, hardness, softness, electronegativity, and electrophilicity indexes), the ADME and toxicity related risks profiles were computed as complementary indicators to the final success of a drug candidate. The outcomes of the research pave the way for a better exploitation of the flavonoids in the field of chemistry, biology and food sciences.

MATERIAL AND METHODS

Molecular geometry optimization. The six flavonoid chemical structures were selected for theoretical investigations based on: (i) the chemical

structure diversity and (ii) the potential influence of substituents on the agonistic activity. The 3D geometries were downloaded from PubChem database¹⁴ and preoptimized with a molecular mechanic force field (MMFF94) and semiempirical AM1 methods using Semiempirical¹⁵ module of Schrodinger package. In order to assess different aspects of the electronic structure of the molecule and to calculate various electronic properties, the geometry of the molecule need to be optimized at a specific level of theory. Complete geometric optimization of the AM1 geometries was obtained by applying hybrid DFT¹⁶ with the B3LYP/6-311++ level of theory of Jaguar module. The geometry was optimized without imposing any molecular symmetry constraints. Further, frequency calculations were done to check if there were true minima. The true energies minima of the studied compounds were confirmed by the absence of any imaginary frequency modes. Based on DFT theory several electronic properties such as, *e.g.*, heat of formation (ΔH_f^θ),¹⁷ HOMO and LUMO energies,^{18,19} energy gap (ΔE),^{18,19} hardness (η),^{20,21} softness (σ),²² electrophilicity index (ω),²² electronegativity index (λ),²³ atomic Fukui indices,^{18,19} chemical potential (μ)²⁴ were computed using Jaguar¹⁶ module. The outlines of the calculated quantum chemical properties provide additional mechanistic information about the activity of the studied compounds.

Global and local reactivity descriptors. To describe the reactivity behavior of the studied compounds, 7,8-DHF and five analogs global reactivity descriptors were computed within the DFT framework. The descriptors were calculated according to the equations:

$$IP \sim -E_{\text{HOMO}} \quad (1)$$

$$EA \sim -E_{\text{LUMO}} \quad (2)$$

$$\mu = -(IP + EA)/2 = (E_{\text{HOMO}} + E_{\text{LUMO}})/2 \quad (3)$$

$$\chi = (IP - EA)/2 = -(E_{\text{HOMO}} - E_{\text{LUMO}})/2 \quad (4)$$

$$\eta = IP - EA = E_{\text{LUMO}} - E_{\text{HOMO}} \quad (5)$$

$$S = 1/\eta \quad (6)$$

$$\omega = \mu^2/2\eta \quad (7)$$

The heat of formation (ΔH_f^θ)¹⁷ is defined as an important indicator regarding the thermodynamic stability or instability of compound.

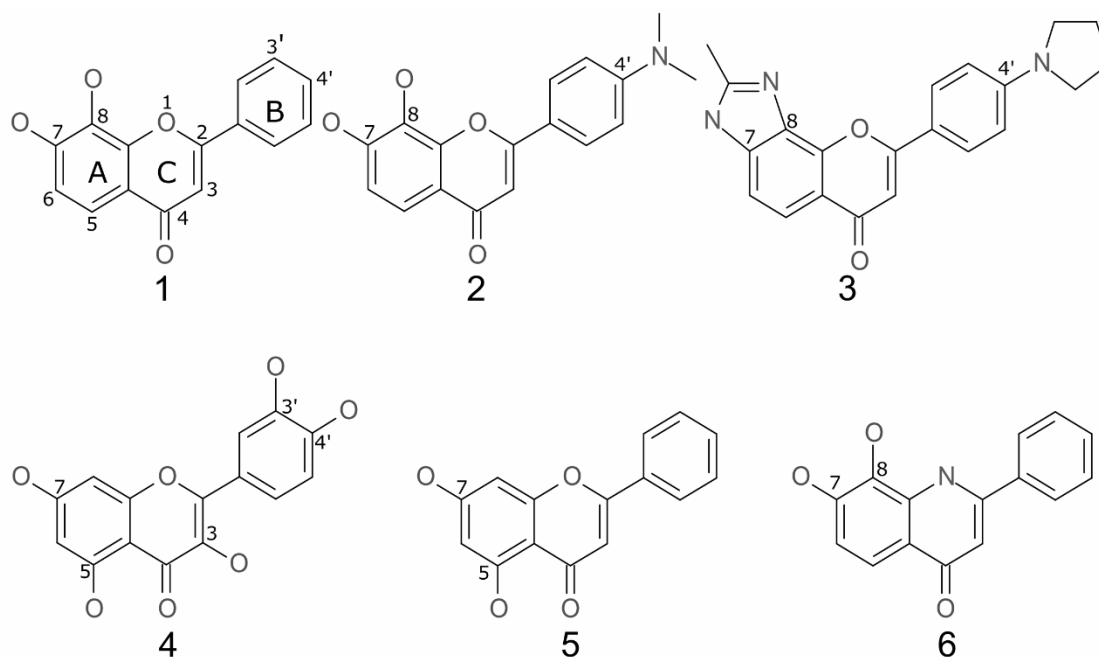


Fig. 1 – Chemical structures of the six flavonoid derivatives: **1** (7,8-dihydroxy-2-phenylchromen-4-one; 7,8-dihydroxyflavone (7,8-DHF)), **2** (2-[4-(dimethylamino)phenyl]-7,8-dihydroxychromen-4-one; 4'-dimethylamino-7,8-dihydroxyflavone (4'-DMA-7,8-DHF)), **3** (2-methyl-8-(4-pyrrolidin-1-ylphenyl)-3H-pyrano[2,3-e]benzimidazol-6-one; 4'-Pyr-7,8-CHR), **4** (2-(3,4-dihydroxyphenyl)-3,5,7-trihydroxychromen-4-one; quercetin (Qu)), **5** (5,7-dihydroxy-2-phenylchromen-4-one; chrysin (5,7-DHF)), **6** (7,8-dihydroxy-2-phenyl-1H-quinolin-4-one; 7,8-DNF); Compound code: Compound number (IUPAC name; short name).

HOMO and LUMO orbitals, the highest occupied molecular orbital (HOMO) and the lowest unoccupied molecular orbital (LUMO), are considered key players in the chemical reactivity and stability of a molecule.^{18,19} According to Koopmans' theorem,²⁵ E_{HOMO} approximates the ionization potential (IP) while the electron affinity (EA) is approximated by E_{LUMO} . The HOMO and LUMO energies and the LUMO-HOMO gap (ΔE)^{18,19} were used as indicators of the kinetic stability of the molecule. A large value of ΔE implies high stability for the molecule and lower reactivity in chemical reactions whereas a small ΔE supposes a low stability and higher molecular reactivity.^{19,26} Ionization potential (IP)²⁴ and electron affinity (EA)²⁴ can estimate the system predisposition of donating or accepting electrons. Chemical potential (μ)²⁴ measures the tendency of a particle to diffuse. Electronegativity²³ (χ), the negative of chemical potential, describes the tendency of an atom to attract electrons (or electron density) towards itself. The global hardness (η),^{20,21} corresponds to the gap between the occupied and unoccupied orbitals. The inverse of hardness is defined as softness (S).²² The electrophilicity index²² (ω) measures the propensity of a species to accept electrons; the larger values of ω indicate higher reactivity of the chemical system.

Atomic Fukui indices (or reactivity indices) and electrostatic potential (ESP) are considered, also, adequate tools for interpreting, predicting and improving the reactive behavior of a molecule.^{18,19} The Fukui indices describe the tendency of an atom into a molecule to lose or accept an electron. The electrostatic potential (ESP)^{27,28} represents a difference in electrical charge between two points and helps to identify the regions of local negative or positive potential in a molecule. The easy way to evaluate HOMO-LUMO orbitals, charge distribution and ESP profiles is to represent it as an electrostatic potential map. To interpret data, a color code was employed, where red represents the lowest ESP value and blue the highest. All these computed reactivity descriptors were visualized with Maestro module of Schrodinger.²⁹

ADME and Toxicity related risk profiles.

The ADME processes play a key role in defining the therapeutic efficacy of a drug candidate. Therefore, the optimization of the lead candidate structure with respect to the ADME processes has become a pivotal part of the drug discovery.³⁰ In this regard, the ADME properties of all six derivatives were predicted using QikProp module of Schrodinger.³¹ The QikProp predicts the widest variety of pharmaceutically properties such as

molecular weight (MW), QPlogPo/w, QPlogS, QPlogHERG, QPPCaco, QPlogBB, percent human oral absorption (%HOA), and polar surface area (PSA) (Table 2).³¹ In addition, the open-source program Osiris Property Explorer³² was used to estimate the risks of side-effects (tumorigenicity, mutagenicity, irritation, reproduction effectivity) and various drug-relevant properties (cLogP, LogS (solubility), MW and drug-likeness). The toxicity risks predictor indicates fragments within a structure, which presents a potential toxicity risk. The prediction process relies on a precompiled set of the structural fragment (provided by the RTECS database) that give rise to toxicity alerts in case they are encountered in the titled structure.³² Furthermore, the overall drug-score was computed by combining the results of clogP, MW, logS, toxicity risk and drug-likeness. This drug-score indicates a possible drug candidate. The *in silico* drug-relevant properties obtained by QikProp and OSIRIS Property Explorer programs are given in Table 2 and 3, respectively.

RESULTS AND DISCUSSION

Global reactivity descriptors in conjunction with the ADME predictions and toxicity related risk profiles have been successfully calculated to explain the correlation between the chemical features of the molecules and their biological activity.

Electronic parameters. Analyzing the values associated with the heat of formation (Table 1) can be easily observed that all compounds apart from compound **3** (4'-Pyr-7,8-CHR), have negative ΔH_f° values, therefore the compounds are stable. Regarding the compound **3**, the positive ΔH_f° value suggests a relatively unstable compound which may react or rapidly decompose into their elements. This is supported by the ESP plot for compound **3** (Fig.2), which presents a large area of positive values (blue shades) near to the 4'-pyrrole ring. The presence of 4'-pyrrole unit on the B-ring instead of the 3',4'-OH groups and of imidazole unit on the A-ring instead of 7,8-OH groups could be also associated with this relative instability. Based on this affirmation, the trends for stability or instability of compounds and the H-donating capacity correspond to the arrangement: 4>5>1>2>6>3. The electron donating ability of a molecule can be predicted also by the HOMO values; a high HOMO value reflects a strong capacity to donate electrons. The HOMO and

LUMO frontier orbitals (EA and IP, respectively) calculated for the six flavonoid analogs at the B3LYP/6-31G** level are drawn in Fig. 2 and the frontier orbital energies are also listed in Table 1. It can be seen from Table 1 that compound **2** (4'-DMA-7,8-DHF) and **3** (4'-Pyr-7,8-CHR) possess the highest HOMO values among the six analogs suggesting a strong electron-donating capability and susceptibility to an electrophilic attack for the molecules. The HOMO values of compounds which possess one nitrogen atom in the molecule (compounds **2** (4'-DMA-7,8-DHF), and **6** (7,8-DNF)) are in the same range of values implying almost the same capability to donate electrons. The presence of more than one nitrogen atom in molecule reduces the HOMO and LUMO values, the case of compound **3**. When comparing the electronic features computed for compounds **1** and **6**, it can be concluded that the replacement of the O-atom with the NH-group alters the descriptors values and implicitly diminishes the agonistic activity. The LUMO values indicated that two out of six analogs (compounds **1** and **5**) are the most electrophilic compounds and possible with higher agonistic effect. Looking at Fig. 2, it can be observed that the HOMO frontier orbitals of the four out of six flavonoids (**1**, **4**, **5**, and **6** compounds) are distributed mainly on the A ring and the C2-C3 double bond of the C rings, while the LUMO frontier orbitals are allocated to the B and C rings. The distribution of the HOMO orbitals on the A ring showed that the 7,8-dihydroxy group is essential for the agonistic activity. A deep analysis of the LUMO distribution plots on the B and C rings highlights the importance of the carbonyl (C=O) bond and O-atom within the molecule. This observation is supported by the ESP plots of compounds. All five out of six ESP plots (Fig.2) indicate an electronegative potential region (red shade; excepting compound **6**) near to the oxygen atom and the carbonyl unit of the C ring meaning that this region is susceptible to electrophilic attack. For the case of compounds **2** and **3**, the HOMO and LUMO orbitals are distributed on the same rings suggesting the same ability to donate or attract electrons. This mode of orbitals distribution can be attributed to the presence of positively charged nitrogen atoms in the molecules. The charge distribution plots also correlate with the results of ESP plots. Low ΔE values for compounds **2**, **3** and **4** signifies less stability and probably a higher molecular reactivity comparing to other three compounds.

The Fukui indices plots for all six derivatives (Table 1S (a) and (b) of Supplementary Information) emphasizes the atomic sites susceptible to nucleophilic or/and electrophilic attack. We plotted only the significant values of Fukui indices which correspond to the highest peaks of the Fukui plots. Here, we discussed only the plots corresponding to the 7,8-dihydroxyflavone derivatives (compounds **1**, **2** and **3**). The HOMO Fukui values for compound **1** characterized the O7 and O8 on the A-ring as sensitive to an electrophilic attack while the HOMO Fukui values of the compounds **2**, and **3** suggested the N-atom at 4'-substitution position on the B-ring as more reactive towards an electrophilic attack. The chemical potential (μ), electronic hardness (η), global softness (S), electronegativity (χ) and electrophilicity (ω) descriptors were computed as complementary information for the chemical reactivity of flavonoid analogs. The descriptors values are in good agreement with the calculated electronic features (HOMO-LUMO energies, band gap energies, and ESP results). Taken together, these outcomes emphasize the impetuous presence of the 7,8-dihydroxy groups (on the A ring), the oxygen atom (in the middle of C ring) for the agonistic effect of 7,8-dihydroxyflavone analogs. Additionally, the 4'-substitution unit on the B-ring could influence positively (-dimethylamino or -pyrrolidino group) or negatively (-F or -OH group) the agonistic activity.

ADME analysis and Toxicity related risks profiles. The ADME parameters of all six flavonoids were estimated using QikProp module. The ADME parameters values (Table 2) showed that five out of six compounds fulfilled the ADME properties. The only exception is quercetin (**4**) for

which five out of eight ADME features have lower values close to the inferior limit of the accepted ones. All these shortcomings can be assigned to the presence of the five hydroxyl groups and seven oxygen atoms in the molecule. Analysis of the ADME parameters for the 7,8-dihydroxyflavone analogs (compounds **1**, **2** and **3**) suggested that compound **3** displays an improved ADME profile. It is well known from the literature that the most failures of marketed drugs were related to the hERG inhibition.^{33,34} In this case, all three derivatives fall within the accepted range of hERG values with compound **3** exhibiting the best value. More interestingly, this compound showed higher percent human oral absorption (e.g. 100%), Caco-2 cell permeability, QPlogPo/w and QPlogS as compared to values of compounds **1** and **2**.

The OSIRIS calculations are used mainly in drug development for identifying the mutagenic and tumorigenic potentials of the chemical candidates.³² Results of the OSIRIS calculations indicated that the analog **3** (4'-Pyr-7,8-CHR) has no mutagenic and tumorigenic potential. Compounds **1** and **2** are showing high risks of undesired effects like mutagenicity and tumorigenicity, respectively. Among the three 7,8-dihydroxyflavone analogs (compounds **1**, **2** and **3**), compound **3** showed the highest values of drug-likeness and drug score. This behavior could be explained by the introduction into the molecule of the pyrrole and imidazole rings. Both undesirable effects, namely mutagenicity, and tumorigenicity were assigned to quercetin (**4**). The ADME analysis in conjunction with OSIRIS results suggested compound **3** as possible TrkB agonist agent with enhanced pharmacological features as compared to the previously analyzed compounds. Our pharmacokinetics results are in accordance with the *in vitro* ADME profile examined by Liu *et al.*^{11,12}

Table 1

The calculated electronic features heat of formation, HOMO and LUMO energies, ΔE , the chemical potential (μ), electronic hardness (η), global softness (S), electronegativity (χ) and electrophilicity index (ω), for all six flavonoids

ID _{Compound}	1	2	3	4	5	6
HF (kcal/mol)	-80.9367	-69.0312	47.0262	-207.858	-85.2376	-52.9005
E _{Homo} (eV)	-6.033	-5.188	-5.042	-5.643	-6.0004	-5.503
E _{Lumo} (eV)	-1.792	-1.253	-1.112	-1.679	-1.886	-1.296
ΔE	4.241	3.935	3.93	3.964	4.114	4.207
χ (eV)	3.913	3.221	3.077	3.661	3.943	3.400
η (eV)	4.241	3.935	3.93	3.964	4.114	4.207
S (eV)	0.236	0.254	0.254	0.252	0.243	0.238
μ (eV)	-3.913	-3.221	-3.077	-3.661	-3.943	-3.400
ω (eV)	1.805	1.318	1.205	1.691	1.89	1.374

Table 2

ADME parameters prediction for all six flavonoids using QikProp³¹ module

ID	MW	PSA ^a	QPlogPo/w ^b	QPlogS ^c	QPPCaco ^d	QPlogBB ^e	QPlogHERG ^f	%HOA ^g
1	254.24	78.687	1.950	-3.286	384.650	-0.830	-5.166	84.629
2	297.31	82.034	2.273	-4.094	369.371	-1.032	-5.272	86.208
3	345.40	66.961	3.848	-6.302	1113.01	-0.472	-5.984	100
4	302.24	143.172	0.382	-2.889	18.928	-2.388	-5.075	52.042
5	254.24	77.341	2.374	-3.613	388.013	-0.867	-5.224	87.183
6	253.26	82.767	1.641	-3.036	325.777	-1.011	-5.282	81.530

^a the polar surface area <math> < 140\text{\AA}^2 </math>, ^b the predicted octanol/water partition coefficient, logP (acceptable range -2 to 6.5), ^c the predicted aqueous solubility, logS; S in mol dm⁻³ (acceptable range -6.5 to 0.5), ^d predicted apparent Caco-2 cell permeability in nm/sec (acceptable range: <math> < 25 </math> poor, > 500 great), ^e the predicted brain/blood partition coefficient, (acceptable range: -3.0 to 1.2), ^f the predicted IC50 value for blockage of HERG K⁺ channels, (acceptable range: below -5), ^g the predicted human oral absorption on 0 to 100% scale, (acceptable range: <math> < 25\% </math> poor, $> 80\%$ high)

Table 3

The drug-like and toxicity related risks profiles of the six flavonoids predicted by OSIRIS Property Explorer

ID	1	2	3	4	5	6
TPSA	66.76	70	58.22	127.4	66.76	69.56
Drug-likeness	0.89	0.55	3.86	1.60	0.97	0.50
Drug-score	0.44	0.42	0.69	0.30	0.75	0.82
Toxicity risk	■ mutagenic	● mutagenic	● mutagenic	■ mutagenic	● mutagenic	● mutagenic
	● tumorigenic	■ tumorigenic	● tumorigenic	■ tumorigenic	● tumorigenic	● tumorigenic
	● irritant	● irritant	● irritant	● irritant	● irritant	● irritant
	● reproductive effective	● reproductive effective	● reproductive effective	● reproductive effective	● reproductive effective	● reproductive effective

*the red color squares indicate properties with high risks of undesired effects like mutagenicity or tumorigenicity whereas the green color circles indicate drug-conform behavior.

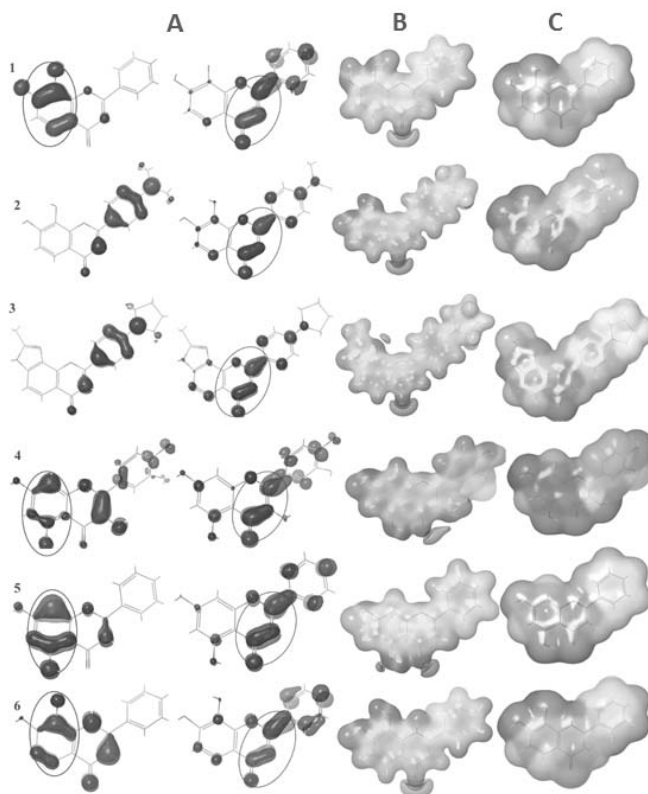


Fig. 2 – The three-dimensional HOMO and LUMO orbitals (A), electrostatic potential profiles (B) and charge distributions (C) of the six flavonoid optimized structures.

CONCLUSIONS

A systematic computational study on the properties of six 7,8-dihydroxyflavone derivatives has been carried out to get deeper insights into their molecular properties responsible for the agonistic effect to TrkB receptor. In this light, the AM1 and DFT calculations in conjunction with the ADME and toxicity related risks predictions were used to explore the structural features and pharmacological profile. Our results showed that 7,8-dihydroxy groups (on the A ring) and the oxygen atom (in the middle of C ring) are essential for the agonistic activity to TrkB receptor. Additionally, the 4²-position at the B-ring could be important for agonistic activity. The ADME and OSIRIS analysis revealed that compound **3** (2-methyl-8-(4-pyrrolidin-1-ylphenyl)-3H-pyrano[2,3-e]benzimidazol-6-one) have enhanced pharmacological properties as compared to the original 7,8-dihydroxyflavone. Hence, our theoretical results are in accordance with the experimental studies presented by Liu *et al.*^{11,12}

Acknowledgements: This paper was published under the frame of the Project 1.2, Theme 1.2.2 of the Institute of Chemistry Timișoara of the Roumanian Academy and of strategic grant of the Romanian National Authority for Scientific Research and Innovation, CNCS -UEFISCDI, project number PN-II-RU-TE-2014-4-0422.

REFERENCES

1. A. N. Panche, A. D. Diwan and S. R. Chandra, *J. Nutr. Sci.*, **2016**, *5*, e47.
2. D. F. Romagnolo and O. I. Selmin, *J. Nutr. Gerontol. Geriatr.*, **2012**, *31*, 206-238.
3. I. C. Arts, D. R. Jacobs, Jr., M. Gross, L. J. Harnack and A. R. Folsom, *Cancer Causes Control*, **2002**, *13*, 373-382.
4. E. Linos and W. C. Willett, *J. Natl. Compr. Canc. Netw.*, **2007**, *5*, 711-718.
5. S. Kumar and A. K. Pandey, *Sci. World J.*, **2013**, *29*, ID162750.
6. C. Hui, X. Qi, Z. Qianyong, P. Xiaoli, Z. Jundong and M. Mantian, *PLoS One*, **2013**, *8*, e54318.
7. E. Middleton, *Trends Pharmacol. Sci.*, **1984**, *5*, 335-338.
8. K. R. Narayana, M. S. Reddy, M. R. Chaluvadi and D. R. Krishna, *Indian J. Pharmacol.*, **2001**, *33*, 2-16.
9. S. W. Jang, X. Liu, M. Yepes, K. R. Shepherd, G. W. Miller, Y. Liu, W. D. Wilson, G. Xiao, B. Bianchi, Y. E. Sun and K. Ye, *Proc. Natl. Acad. Sci. USA.*, **2010**, *107*, 2687-2692.
10. Y. Zeng, F. Lv, L. Li, H. Yu, M. Dong and Q. Fu, *J. Neurochem.*, **2012**, *122*, 800-811.
11. X. Liu, C. B. Chan, S. W. Jang, S. Pradoldej, J. Huang, K. He, L. H. Phun, S. France, G. Xiao, Y. Jia, H. R. Luo and K. Ye, *J. Med. Chem.*, **2010**, *53*, 8274-8286.
12. X. Liu, C.B. Chan, Q. Qi, G. Xiao, H.R. Luo, X. He and K. Ye, *J. Med. Chem.*, **2012**, *55*, 8524-8537.
13. J. Lameira, C. N. Alves, V. Moliner and E. Silla, *Eur. J. Med. Chem.*, **2006**, *41*, 616-623.
14. PubChem database, <https://pubchem.ncbi.nlm.nih.gov/search/search.cgi>
15. Semi-empirical NDDO module, version 10.3, 2017, Schrödinger, LLC, New York, N.Y.
16. Jaguar, version 9.6, 2017, Schrödinger, LLC, New York, N.Y.
17. B. W. Clare, *J. Mol. Struct. -Theochem.*, **1995**, *337*, 139-150.
18. I. Fleming, "Molecular Orbitals and Organic Chemical Reactions", 1st edition, I. Fleming (Ed.), John Wiley & Sons, New York, 2010, p.526
19. Z. Zhou and R. G. Parr, *J. Am. Chem. Soc.*, **1990**, *112*, 5720-5724.
20. P. W. Ayers and R. G. Parr, *J. Am. Chem. Soc.*, **2000**, *122*, 2010-2018.
21. R. G. Pearson, *J. Chem. Educ.*, **1987**, *64*, 561-567.
22. P. K. Chattaraj, B. Maiti and U. Sarkar, *J. Phys. Chem.*, **2003**, *107*, 4973-4975.
23. R. G. Parr, R. A. Donnelly, M. Levy and W. E. Palke, *J. Chem. Phys.*, **1978**, *68*, 3801-3807.
24. R. G. Pearson, *J. Chem. Sci.*, **2005**, *117*, 369-377.
25. T. A. Koopmans, *Physica*, **1933**, *1*, 104-113.
26. R. G. Pearson, *Proc. Nat. Acad. Sci. USA*, **1986**, *83*, 8440-8441.
27. J.S. Murray, F. Abu-Awwad and P. Politzer, *J. Mol. Struct. (Theochem)*, **2000**, *501*, 241-250.
28. P. Politzer and J. S. Murray, *Theor. Chem. Acc.*, **2002**, *108*, 134-142.
29. Maestro, version 11.2, 2017, Schrödinger, LLC, New York, N.Y.
30. H. Pajouhesh and G. R. Lenz, *NeuroRx*, **2005**, *2*, 541-553.
31. QikProp, version 5.2, 2017, Schrödinger, LLC, New York, N.Y.
32. Organic Chemistry Portal, 2016, <http://www.organic-chemistry.org/prog/peo/>
33. M. C. Sanguinetti and M. Tristani-Firouzi, *Nature*, **2006**, *440*, 463-469.
34. W. S. Redfern, L. Carlsson, A. S. Davis, W. G. Lynch, I. MacKenzie, S. Palethorpe, P. K. Siegl, I. Strang, A. T. Sullivan, R. Wallis, A. J. Cammand and T. G. Hammond, *Cardiovasc Res.*, **2003**, *58*, 32-45.

